Clin Proteom (2010) 6:29–41
DOI 10.1007/s12014-010-9041-4

Characterization of Nitrotyrosine-Modified Proteins in Cerebrospinal Fluid

Ashley S. Beasley · Caroline Anderson · Justin McArthur · Ned Sacktor · Avindra Nath · Robert J. Cotter

Published online: 11 March 2010

Abstract
Background HIV-associated neurocognitive disorders (HAND) has been associated with the up-regulation of various oxidative stress pathways. Previous studies have linked the neuronal damage observed in individuals diagnosed with HAND to increased nitrotyrosine modification of neuronal proteins.
Materials and methods Tyrosine nitration alters protein structure and function, affects biological half-life, and potentially prevents the phosphorylation of key tyrosine residues involved in signal transduction pathways. Therefore, in this study we employed proteomics-based experimental approaches to investigate nitrotyrosine-modified proteins in pooled cerebrospinal fluid (CSF) of individuals diagnosed with HAND. To identify specific nitrotyrosine-modified proteins in the CSF of individuals diagnosed with HAND, affinity purification and high-performance tandem mass spectrometry are utilized in a "bottom-up" proteomics approach.
Results From tandem mass spectrometric analysis, we identified major proteins that underwent nitration as a result of nitro-oxidative stress in the CSF of individuals diagnosed with HAND. We also utilized analytical and biochemical techniques to characterize the expression and modification site of in vivo nitrated lipocalin-type prostaglandin-D synthase in HAND CSF.

Keywords BSA · CSF · HIV · HAND · Oxidative stress · Tyrosine nitration

Abbreviations

BSA	Bovine Serum Albumin
CSF	Cerebrospinal fluid
HIV	Human Immunodeficiency Virus
HAND	HIV-associated neurocognitive disorders
L-PGDS	Lipocalin-type prostaglandin-D synthase
PTM	Post-translational modification
$ONOO^-$	Peroxynitrite

Introduction

During the initial phases of human immunodeficiency virus (HIV) infection, the virus penetrates the blood-brain barrier and invades the host central nervous system (CNS). This leads to a cascade of intracellular anti-viral events including the production of oxidative stress that facilitate the control of viral replication and production [1]. The over production of these anti-viral responses have been linked to various neurological complications due to neuronal damage and toxicity, such as HIV-associated neurocognitive disorders (HAND) [1, 2]. However, with the advent of highly active antiretroviral therapy (HAART) the incidence and severity of HAND has drastically decreased but the prevalence of

Electronic supplementary material The online version of this article (doi:10.1007/s12014-010-9041-4) contains supplementary material, which is available to authorized users.

A. S. Beasley · R. J. Cotter (✉)
Pharmacology and Molecular Sciences,
Johns Hopkins University School of Medicine,
725 North Wolfe Street, Biophysics Building, B7,
Baltimore, MD 21205, USA
e-mail: rcotter@jhmi.edu

C. Anderson · J. McArthur · N. Sacktor · A. Nath
Neurology, Johns Hopkins University School of Medicine,
725 North Wolfe Street, Biophysics Building, B7,
Baltimore, MD 21205, USA

A. Nath
Neuroscience, Johns Hopkins University School of Medicine,
725 North Wolfe Street, Biophysics Building, B7,
Baltimore, MD 21205, USA

HAND has increased [3]. HAART has reduced the viral load, significantly improved the $CD4^+$ T-cell counts, and extended the life expectancy of individuals infected with HIV. Consequently, the life expectancy benefits associated with HAART and the low turnover of HIV-infected cells in the CNS has led to the progressive rise in milder HIV-associated cognitive disorders. Little is known about the mechanisms and pathways associated with the development and progression of HAND; therefore, current diagnosis of HAND requires extensive neuropsychological testing. Although the mechanism of development of HAND is unknown, previous studies of individuals diagnosed with HAND have shown a correlation between the degree of severity of HAND and elevated levels of inducible nitric oxide synthase (iNOS) [4]. The enzymatic activity of iNOS leads to the production of nitric oxide (NO), which can act as a cytotoxic effector molecule or a pathogenic mediator when produced at high rates [5]. Elevated levels of free reactive nitrogen species interact with neuronal proteins and lead to the selective nitration of tyrosine residues. Protein tyrosine nitration is a dynamic and selective post-translational modification that is a well-established biomarker of oxidative stress. Nitrotyrosine is the product of the uncatalyzed reaction of a tyrosine residue and peroxynitrite ($ONOO^-$), which is a powerful oxidant produced from the reaction of NO and superoxide (Fig. 1). In addition to the uncatalyzed reaction, catalyzed reactions of $ONOO^-$ with CO_2, transition metals, and myeloperoxidase can also lead to the formation of nitrotyrosine [6]. Tyrosine nitration alters protein structure and function, affects biological half-life, solubility, and increases the degree of protein degradation [5]. The addition of the bulky $–NO_2$ group also imposes steric restrictions on the tyrosine aromatic ring which can lead to the inhibition of phosphorylation of the phenolic hydroxyl group of the phenolic ring

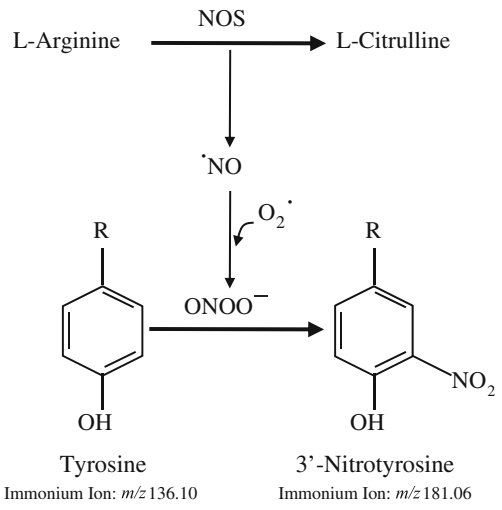

Fig. 1 Tyrosine nitration pathway

of tyrosine [6]. Therefore, characterization of nitrotyrosine-modified proteins in cerebrospinal fluid (CSF) offers unique opportunity for the identification of key proteins that contribute to the HIV-induced effects of neurological dysfunction.

In this study, we employ affinity-based purification and high-performance tandem mass spectrometry in a "bottom-up" proteomics approach to investigate nitrotyrosine-modified proteins in the CSF of individuals diagnosed with HAND.

Materials and Methods

In vitro nitration of BSA and L-PGDS One milligram of bovine serum albumin (BSA; Sigma, St. Louis, MO; and Sigma) was incubated with a 1.54 mM (100 μL) solution of peroxynitrite (Upstate, Lake Placid, NY) in 0.3 M NaOH for 45 min at room temperature. Following nitration, the peroxynitrite-treated BSA (*n*-BSA) solution was desalted with protein desalting spin columns (Pierce, Rockford, IL).

High-Performance Liquid Chromatography Analysis The desalting spin column flowthrough fraction was used to validate in vitro peroxynitrite-treated BSA. One hundred microliters of *n*-BSA (100 μg) in 0.1% trifluoroacetic acid (TFA) was injected onto a 250×2.0 mm Jupiter 5 μ C_4 300A (Phenomenex, Torrance, CA) reversed-phase column. The aqueous mobile phase A consisted of 0.1% TFA in water (Solvent A) and the organic mobile phase consisted of 0.1% TFA in ACN (Solvent B). The nitrated and non-nitrated protein was eluted with the following gradient: 30% Solvent B at 0–5 min, 50% Solvent B at 35 min, 100% Solvent B at 40 min, and 3% Solvent B at 50 min. The absorbance was monitored at both 214 and 350 nm.

CSF Specimens The human CSF samples were obtained from non-HIV-infected and HAND diagnosed individuals from the Lumbar Puncture Clinic at Johns Hopkins Hospital. The samples were divided into two groups: non-HIV ($n=3$) and HAND ($n=4$). The non-HIV group consisted of two patients with normal pressure hydrocephalus and one with possible multiple sclerosis. None of them had any risk factors for HIV infection. The collected CSF samples were centrifuged at 3,000 rpm for 10 min to remove cellular debris. The cell-free CSF supernatant was stored at −80°C in 1.0 mL aliquots until further analysis to prevent sample degradation. Prior to analysis, the CSF samples were heated at 60°C for 20 min and pooled. Pooling of CSF was necessary since the detailed proteomic analysis required large amounts of CSF. CSF samples from ten individuals were initially screened for nitrotyrosine by slot blot as previously described [7] and the four HAND CSF samples with the highest levels of nitrotyrosine

content were pooled for further analysis. This optimized our chances for detection of nitrotyrosine-modified proteins.

Nitrotyrosine Enrichment Prior to affinity purification of the nitrotyrosine-modified proteins, the control and diseased (HAND) CSF were immunodepleted with the Proteoseek™ antibody-based albumin/IgG removal kit (Pierce, Rockford, IL). Following immunodepletion, the CSF samples were incubated with 100 μg of anti-nitrotyrosine (clone 1A6) agarose conjugate (Upstate, Lake Placid, NY) overnight at 4°C with gentle agitation to maintain optimal distribution of the antibody resin in the protein mixture. The resin was collected by centrifugation at 1,500×*g* for 1 min and washed twice with phosphate buffer saline (PBS, pH 7.4). The nitrated proteins were eluted with 5% (*v/v*) formic acid in water and the fractions were concentrated in a speedvac.

Lipocalin-type Prostaglandin D Synthase Enrichment Co-immunoprecipitation of lipocalin-type prostaglandin D synthase (L-PGDS) was performed according to the Catch and Release v2.0 kit (Upstate, Lake Placid, NY) recommendations. The pooled albumin/IgG depleted CSF samples were incubated with the anti-LPGDS monoclonal antibody (Cayman Chemical, Ann Arbor, MI) at 4°C overnight. Following incubation, the spin column was washed twice with 1× wash buffer and each wash was centrifuged at 5,000 rpm for 1 min. The antigen:antibody complex was eluted from the affinity resin with non-denaturing elution buffer (PBS, pH7.4) and the affinity purification fractions were concentrated in the speedvac and resuspended in 50 μL of PBS (pH7.4). The above procedure was utilized to enrich the nitrotyrosine-modified protein from the LPGDS-enriched CSF samples.

Sodium dodecyl sulfate-polyacrylamide gel electrophoresis The immunoprecipitation fractions were loaded and separated by sodium dodecyl sulfate-polyacrylamide gel electrophoresis (SDS-PAGE) on a NuPAGE 4-12% (*w/v*) Bis-Tris gel (Invitrogen, Carlsbad, CA) and visualized via silver staining [8, 9]. Briefly, the gels were fixed in 50% (*v/v*) ethanol (EtOH)/

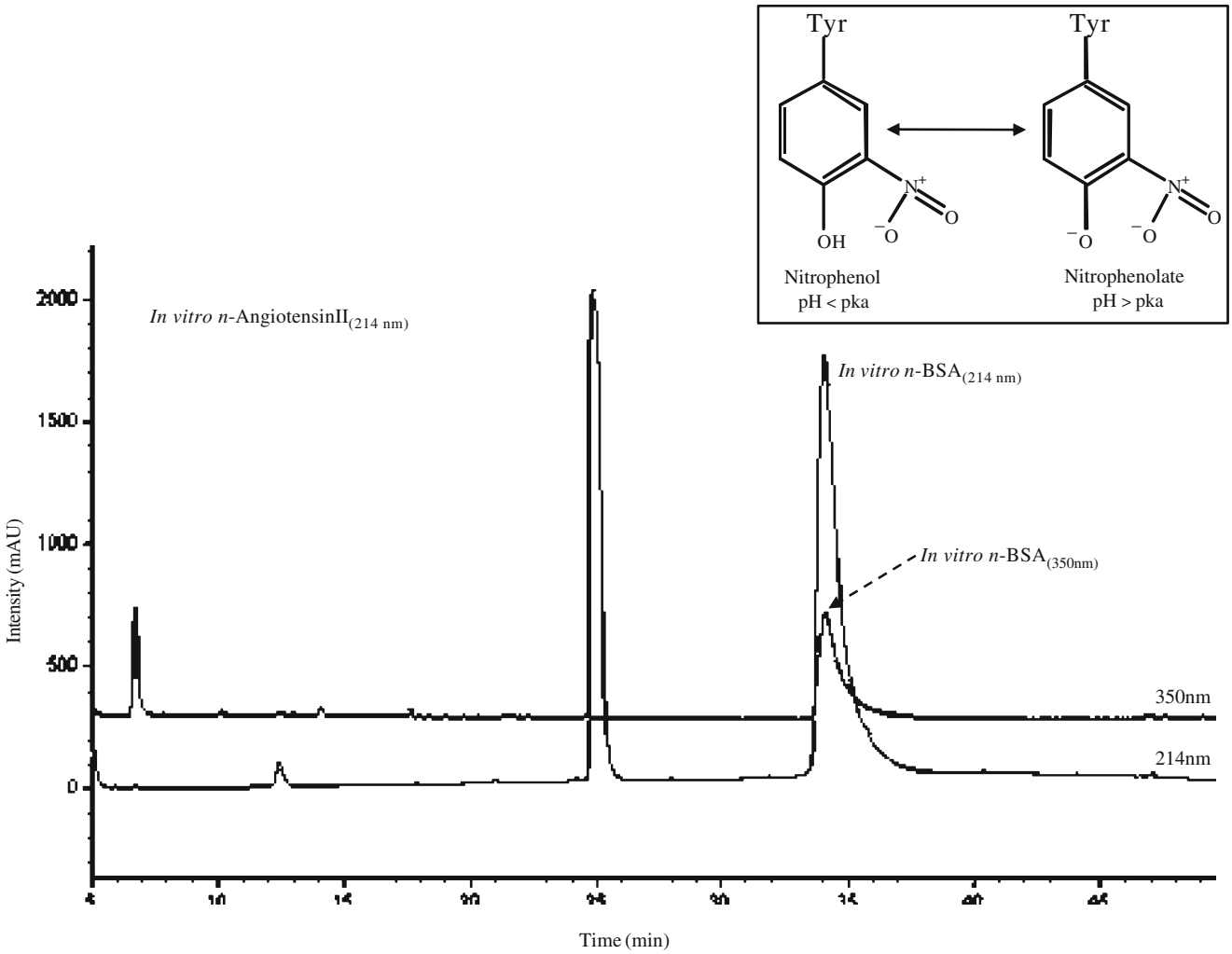

Fig. 2 Reversed-phase LC analysis of in vitro *n*-BSA containing unmodified Angiotensin II (internal non-nitrated standard) at 214 and 350 nm

Table 1 Tryptic products of *in vitro n*-BSA

Peptide sequence	Charge	Peptide ID probability	Mascot Ion score	Mascot identity score	X! Tandem–log(e) score	Observed m/z	Actual peptide mass (AMU)	Calculated +1H peptide mass (AMU)	Actual minus calculated peptide mass (AMU)
TVMENFVAFVDK	2	95.00%	71.6	38	5.02	708.3477	1,414.68	1,415.69	–0.0004417
IETMREKVLTSSAR	3	64.20%	0	0	1.31	546.623	1,636.85	1,636.87	0.9842
DAFLGSFLYEYSR	2	95.00%	41.8	38.3	5.48	806.8712	1,611.73	1,612.73	0.006302
LGEYGFQNALIVR	2	95.00%	86.9	38.6	8.09	762.8956	1,523.78	1,524.78	0.002306
RHPEYAVSVLLR	3	95.00%	47.5	38.8	4.57	495.6044	1,483.79	1,484.80	0.0003256
YLYEIAR	2	65.50%	29.8	36.6	0	486.7436	971.4716	972.4791	0.0004075
YLYEIAR	2	68.90%	30.5	36.6	0	486.7436	971.4716	972.4791	0.0004075
YLYEIAR	2	85.30%	35.6	36.5	0	509.2361	1,016.46	1,017.46	0.0003306
AEFVEVTK	2	95.00%	54.1	35.9	0	461.7474	921.4792	922.4886	–0.001529
AEFVEVTK	1	85.60%	43.3	35.9	0	922.4875	921.4797	922.4886	–0.001053
AEFVEVTKLVTDLTK	2	95.00%	0	0	3.44	847.9707	1,693.93	1,692.94	1.991
AFDEK	2	74.70%	29.8	34.4	0	305.1478	608.28	609.2885	–0.0006331
ATEEQLK	1	76.10%	27.9	36.3	0	818.4245	817.4167	818.4261	–0.001546
ATEEQLK	2	95.00%	51.1	36.3	0	409.7164	817.4172	818.4261	–0.001022
CCTKPESER	2	95.00%	64.7	36.6	1.48	526.7297	1,051.44	1,052.45	0.001065
CCTKPESER	3	95.00%	30.8	36.6	2	351.489	1,051.44	1,052.45	0.0008892
DAFLGSFLYEYSR	2	95.00%	79	38.3	8.03	784.3771	1,566.74	1,567.74	0.003179
DAFLGSFLYEYSRR	3	95.00%	26.8	45.6	1.74	575.2875	1,722.84	1,723.84	0.002598
DAIPENLPPLTADFAEDK	2	95.00%	50.8	46.3	5	978.4852	1,954.95	1,955.96	0.002055
DLGEEHFK	2	95.00%	51.1	36.6	0	487.7336	973.4516	974.4585	0.0009688
DTHKSEIAHR	3	95.00%	43.9	43.9	1.7	398.5388	1,192.59	1,193.60	–0.001902
FKDLGEEHFK	2	95.00%	59.3	37.6	3.72	625.3146	1,248.61	1,249.62	–0.0004376
FKDLGEEHFK	3	95.00%	59.6	37.6	3.96	417.2124	1,248.61	1,249.62	–0.0002136
FKDLGEEHFK	4	95.00%	27.5	37.5	1.29	313.1605	1,248.61	1,249.62	–0.00319
FPKAEFVEVTK	2	68.50%	0	0	1.85	648.3491	1,294.68	1,294.70	0.9857
FPKAEFVEVTK	3	95.00%	27.3	38.1	1.12	432.2374	1,293.69	1,294.70	–0.008115
FQNALLVR	2	93.50%	44.8	44	0	480.7861	959.5566	960.5631	0.001377
HLVDEPQNLIK	2	95.00%	52.2	38.1	5.66	653.3591	1,304.70	1,305.72	–0.006416
HLVDEPQNLIK	3	95.00%	39.1	38.1	1.27	435.9096	1,304.71	1,305.72	–0.003592
HPEYAVSVLLR	2	95.00%	40.1	38.1	2.08	642.3597	1,282.70	1,283.71	0.0004832
HPEYAVSVLLR	3	95.00%	47.3	38.1	3.68	428.5756	1,282.70	1,283.71	0.0001072
IETMR	1	58.40%	18.1	34.9	0	649.3345	648.3267	649.3344	0.0001521
IETMR	2	77.10%	31	34.9	0	325.1712	648.3268	649.3344	0.0002761
KQTALVELLK	2	95.00%	77	38.8	0	571.8612	1,141.71	1,142.72	–0.0004154

KQTALVELLK	3	95.00%	58.5	38.8	0	381.5762	1,141.71	1,142.72	–0.001991
KVPQVSTPTLVEVSR	2	95.00%	94.1	39.8	7.64	820.4717	1,638.93	1,639.94	–0.002713
KVPQVSTPTLVEVSR	3	95.00%	76.8	39.8	5.64	547.319	1,638.93	1,639.94	0.003111
LCVLHEK	2	95.00%	47	35.7	0	421.232	840.4484	841.4607	–0.004421
LGEYGFQNALIVR	2	95.00%	85.2	38.8	5.66	740.4017	1,478.79	1,479.80	–0.0004167
LSQKFPK	2	95.00%	43.7	36.5	0	424.2566	846.4976	847.5043	0.001177
LSQKFPKAEFVEVTK	3	95.00%	0	0	2.59	584.9897	1,751.95	1,750.97	1.979
LSQRFPK	2	93.40%	43.9	43.2	0	438.2521	874.4886	875.5104	–0.01393
LVNELTEFAK	1	95.00%	33.6	37.4	4.31	1,163.63	1,162.62	1,163.63	–0.001753
LVNELTEFAK	2	95.00%	74.4	37.4	2.82	582.3201	1,162.62	1,163.63	0.001171
LVNELTEFAKTCVADES HAGCEK	3	95.00%	34.7	40.1	2.54	832.05	2,493.13	2,494.16	–0.02511
LVTDLTK	1	79.70%	34.6	36.3	0	789.4715	788.4637	789.4724	–0.0008407
LVTDLTK	2	95.00%	53.2	36.3	0	395.2392	788.4628	789.4724	–0.001717
LVVSTQTALA	2	95.00%	68.3	37.2	3.44	501.795	1,001.57	1,002.58	–0.001308
QTALVELLK	2	95.00%	77.3	37.6	0	507.8132	1,013.61	1,014.62	–0.001414
RHPEYAVSVLLR	2	95.00%	0	0	4.51	720.9116	1,439.81	1,439.81	1.003
RHPEYAVSVLLR	3	95.00%	83.1	38.9	4.43	480.6088	1,438.80	1,439.81	–0.001398
SLHTLFGDELCK	2	95.00%	27.9	44.4	1.74	681.8406	1,361.67	1,362.67	0.000476
TCVADESHAGCEK	2	95.00%	66.3	37.7	6.1	675.2777	1,348.54	1,349.55	0.000973
TCVADESHAGCEK	3	95.00%	44	37.8	2.57	450.5207	1,348.54	1,349.55	–0.000103
TPVSEKVTK	2	95.00%	72.7	43.8	4.43	494.7871	987.5586	988.568	–0.001521
TVMENFVAFVDK	2	95.00%	70.1	38.1	3.43	700.3507	1,398.69	1,399.69	0.0004733
VASLR	2	78.80%	33.1	36.5	0	273.1742	544.3328	545.3411	–0.0004225
VPQVSTPTLVEVSR	2	95.00%	102	39.2	7.68	756.4266	1,510.84	1,511.84	0.002089
YLYEIAR	2	95.00%	45	36.3	0	464.2495	926.4834	927.494	–0.002716

5% (*v/v*) acetic acid in water for a minimum of 30 min, followed by a second fixation step in 50% EtOH for 10 min. The gels were then washed twice for 10 min in water to remove the remaining acid. Prior to staining, the gels were sensitized for 2 min using an aqueous solution of 0.02% (*w/v*) sodium thiosulfate followed by three washes for 5 min each with water to remove the excess sodium thiosulfate. After rinsing, the gels were incubated for 30 min with gentle agitation in chilled 0.1% (*w/v*) silver nitrate. Following staining with silver nitrate, the gels were developed in 2% (*w/v*) sodium carbonate containing 0.037% (*v/v*) formaldehyde in water. The staining reaction was quenched with an aqueous solution of 5% (*v/v*) acetic acid for 5 min. The gels were stored at 4°C in 1% acetic acid in water until further analysis.

Immunoblot Analysis The nitrotyrosine and L-PGDS immunoprecipitation elution fractions were separated by SDS-PAGE on a NuPAGE 4–12% Bis-Tris gel (Invitrogen, Carlsbad, CA). The proteins were then transferred to a polyvinylidene fluoride membrane using the iBlot™ Gel Transfer Device (Invitrogen, Carlsbad, CA) and the SNAP i.d.™ protein detection system (Millipore, Billerica, MA) was used to conduct the immunoblot. The primary antibodies used were mouse monoclonal anti-nitrotyrosine (2 µg/mL; Upstate, Lake Placid, NY) and rat monoclonal anti-L-PGDS (2 µg/mL; Cayman Chemical, Ann Arbor, MI). The respective secondary antibodies (1:5,000 dilution) were goat anti-mouse IgG IRDye® 680 nm (LI-COR Biosciences, Lincoln, NE) and goat anti-rat IgG IRDye® 680 nm (LI-COR Biosciences). The fluorescent blots were imaged on the Odyssey infrared imaging system (LI-COR Biosciences).

In-gel Trypsin Digestion Stained protein bands were excised and destained in 100 µL of destaining solution (1:1

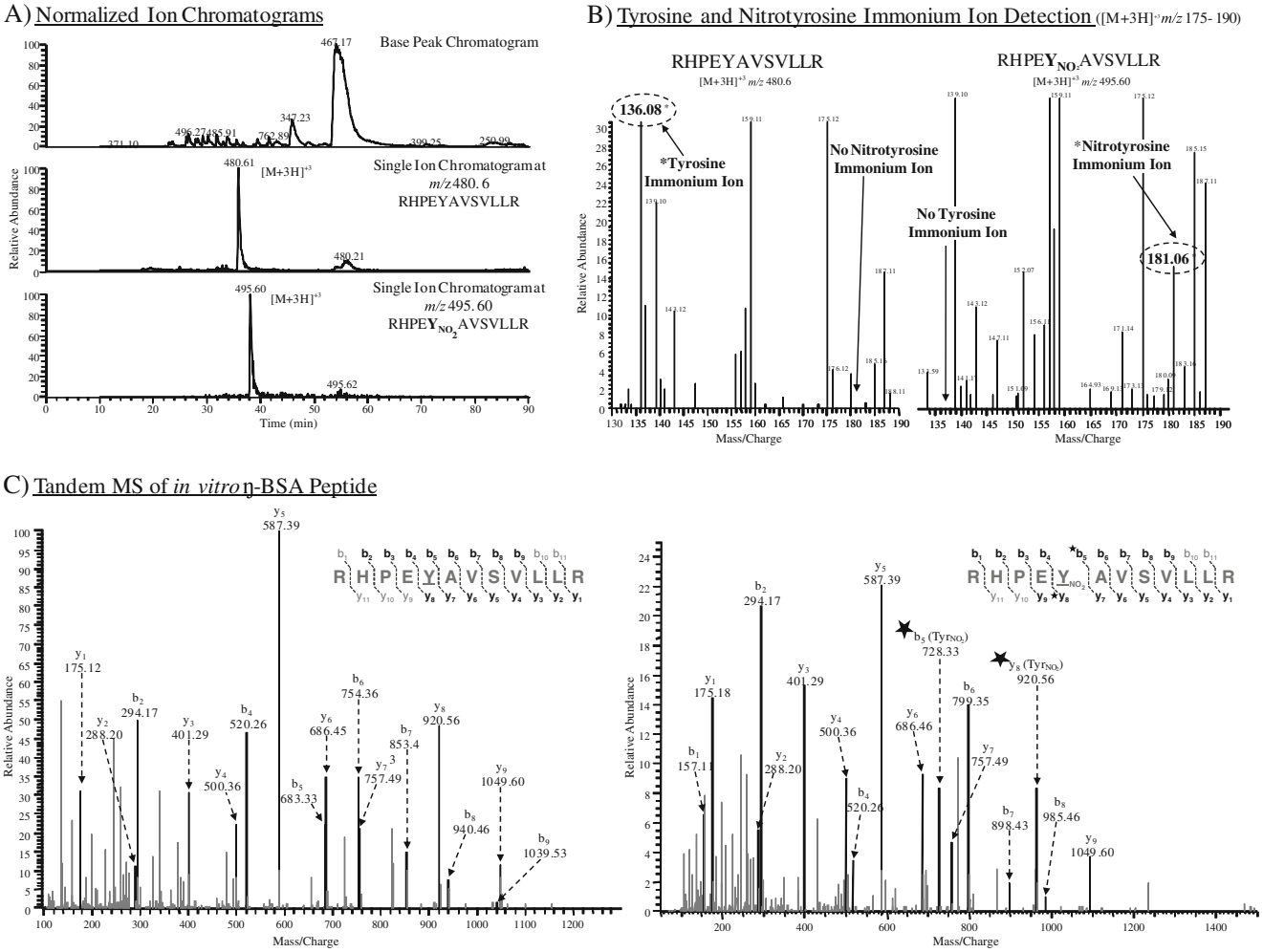

Fig. 3 LTQ-Orbitrap analysis of in vitro *n*-BSA tryptic peptides: RHPEYAVSVLLR and RHPEYNO2AVSVLLR. The base peak ion chromatograms of the MS analysis of the tryptic digestion of in vitro *n*-BSA are presented in Panel A. The single ion chromatograms at *m/z* 480.61 and *m/z* 495.60 represent the detection of the [M+3H]+3 ion of the non-nitrated and nitrated BSA peptide, respectively. The tandem MS spectra of *m/z* 480.61 and *m/z* 495.60 are in Panel C. In addition to changing the peptide mass, the –NO2 group also increases the Tyrosine immonium ion from *m/z* 136.10 to *m/z* 181.06 (Panel B)

mixture of 30 mM potassium ferricyanide: 100 mM sodium thiosulfate) for 10 min. at room temperature. The gel bands were washed with 100 mM ammonium bicarbonate (NH_4HCO_3) and dehydrated with ACN. After drying the bands in the speedvac, pre-selected gel bands were rehydrated in a trypsin solution (10 ng of trypsin in 50 mM NH_4HCO_3) on ice for 45 min. The supernatant was removed and 100 µL of 50 mM NH_4HCO_3 was added to the bands and the bands were placed at 37°C overnight for digestion. The supernatants were removed and the remaining peptides were extracted with 50 µL of 1:1 mixture of ACN and 5% formic acid in water. Following extraction, the peptides were dried in a speedvac and re-suspended in 20 µL of LC-MS loading buffer (3% ACN/ 0.1% formic acid in H_2O) for tandem MS analysis.

NanoLC LTQ-Orbitrap hybrid MS The peptide mixtures were separated by *on-line* reversed-phase (RP) nanoscale capillary liquid chromatography (nano-LC) and analyzed by ESI-tandem MS (LTQ-Orbitrap, Thermo Fisher Scientific, Berman, Germany). Prior to injection onto the reversed-phase column, the sample was injected onto a 10 µL injection loop using the Agilent 1200 nanoflow autosampler (Agilent Technologies, Palo Alto, CA). From the injection loop, the sample was flushed onto the in-house packed fused-silica trap column at a flowrate of 5 µL/min to remove salt and particulate from the peptide mixture. After five washes, the 10-port valve switched from offline to inline with the mobile phase gradient.

For peptide separation, the peptide mixture was injected onto the 12 cm reversed-phase, fused-silica capillary column (ID: 75 µm, packed in-house with C_{18} 5 µm packing material, YMC Europe GmbH) using the Eksigent nanoLC-2D system (Eksigent, Dublin, CA). The aqueous mobile phase consisted of 0.1% formic acid in H_2O (Solvent A) and the organic mobile phase consisted of 0.1% formic acid in ACN (Solvent B). The peptides were eluted from the hydrophobic stationary phase with a linear gradient and the total gradient time was 90 min. Solvent B was held constant at 3% for 5 min, ramped to 10% in 5 min

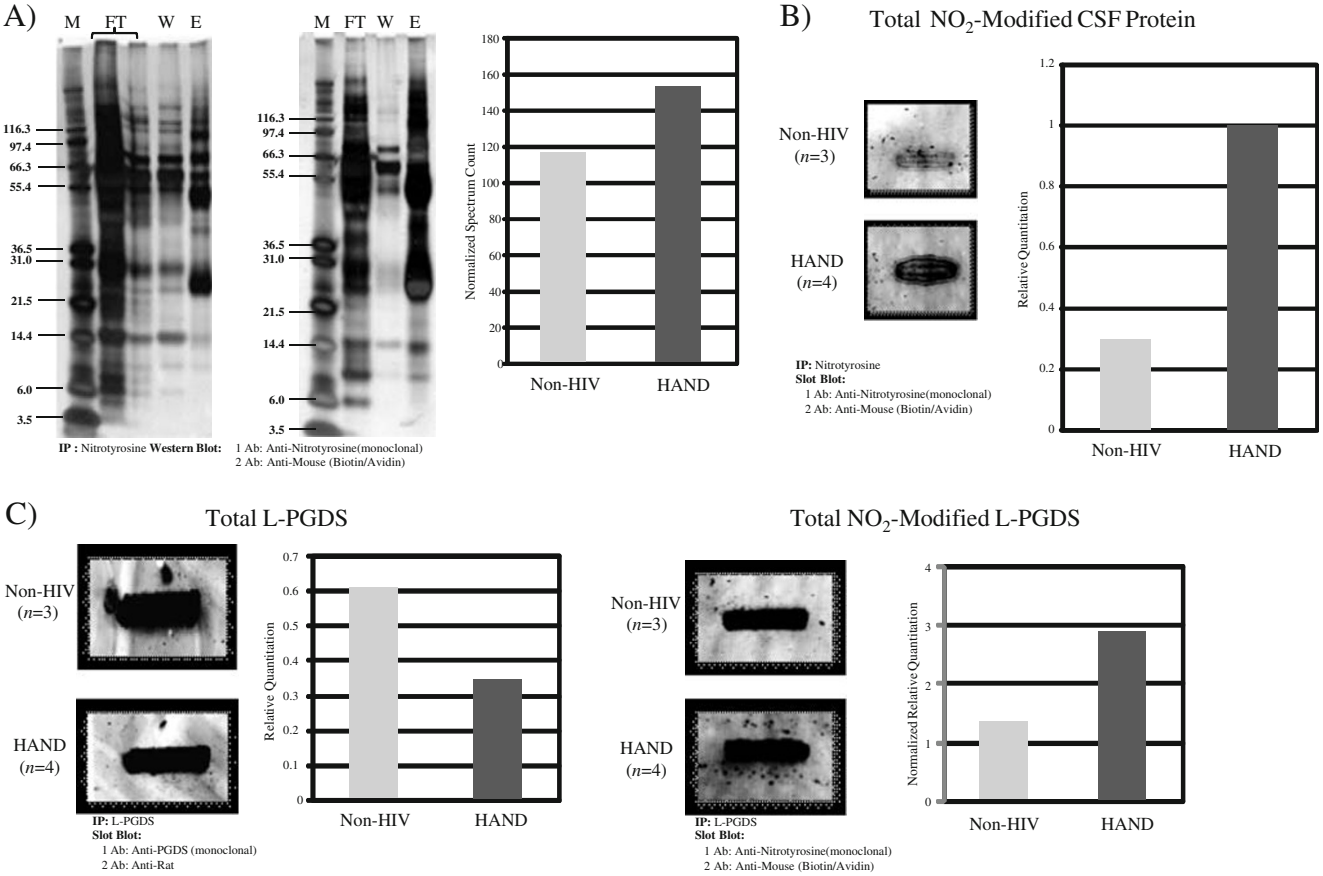

Fig. 4 1-D electrophoresis (**a**) of nitrotyrosine enrichment fractions from pooled non-HIV (control) and HAND CSF. *Lane 1*, MW marker; *lane 2*, flowthrough (non-nitrated proteins); *lane 3*, pre-elution PBS wash; and *lane 4*, 5% formic acid elution (enriched nitrated proteins). The total number of spectra acquired (normalized spectrum count) from Non-HIV (control) and HAND CSF nitrotyrosine-modified sub-proteome (**a**). Quantitative immunoblot analysis of nitrotyrosine content in albumin/IgG-depleted non-HIV (control) and HAND (diseased) CSF (**b**) and L-PGDS (**c**) determined by slot blot analysis

and to 20% in 5 min, followed by an increase to 60% at 60 min. At 80 min, Solvent B was increased to 97% and held constant for 2 min and ramped down to 3% at 85 min to re-equilibrate the reversed-phase column. The eluted peptides were directly transferred from the capillary column to a laser-pulled electrospray ionization emitter tip (New Objective, Woburn, MA) at a spray voltage of 2.0 kV. Data-dependent acquisition was performed on the LTQ-Orbitrap (Thermo Fisher Scientific) mass spectrometer in the positive-ion mode. The survey full MS scans (*m/z* 200–2,000) were acquired in the Orbitrap mass analyzer with a resolution of R=15,000. The four most intense ions from the full MS scan were fragmented with collision-induced dissociation (CID) fragmentation and the MS/MS scans (*m/z* 100–2,000) were also acquired in the Orbitrap with a resolution of R=7,500. The fragmented target ions were dynamically excluded for 90 s. General mass spectrometric conditions were as follows: no sheath and auxiliary gas; ion transfer tube temperature of 200°C; collision gas pressure was 1.5 mTorr; normalized collision energy was 35.0%; ion selection threshold was 10,000; the activation q-value was 0.25; and the activation time was 30 ms.

Database Search and Data Analysis The tandem mass spectra were extracted and the charge state deconvoluted by Mascot Distiller (v. 2.0, Matrix Science). De-isotoping was not performed. The MS/MS samples were analyzed using MASCOT (Matrix Science (version 2.2), London, UK) and X! Tandem (www.thegpm.org; version 2007.01.01.1). The IPI_Human_20060712 protein database (selected for Homo sapiens, version 3.49, 60397 entries) was used by both MASCOT and X! Tandem to search the tandem MS data. For Orbitrap data, a 0.1 Da mass tolerance was allowed for parent ion masses and a 0.5 Da mass tolerance was used for

Table 2 Relative quantification of nitrotyrosine-modified proteins from non-HIV and HAND CSF

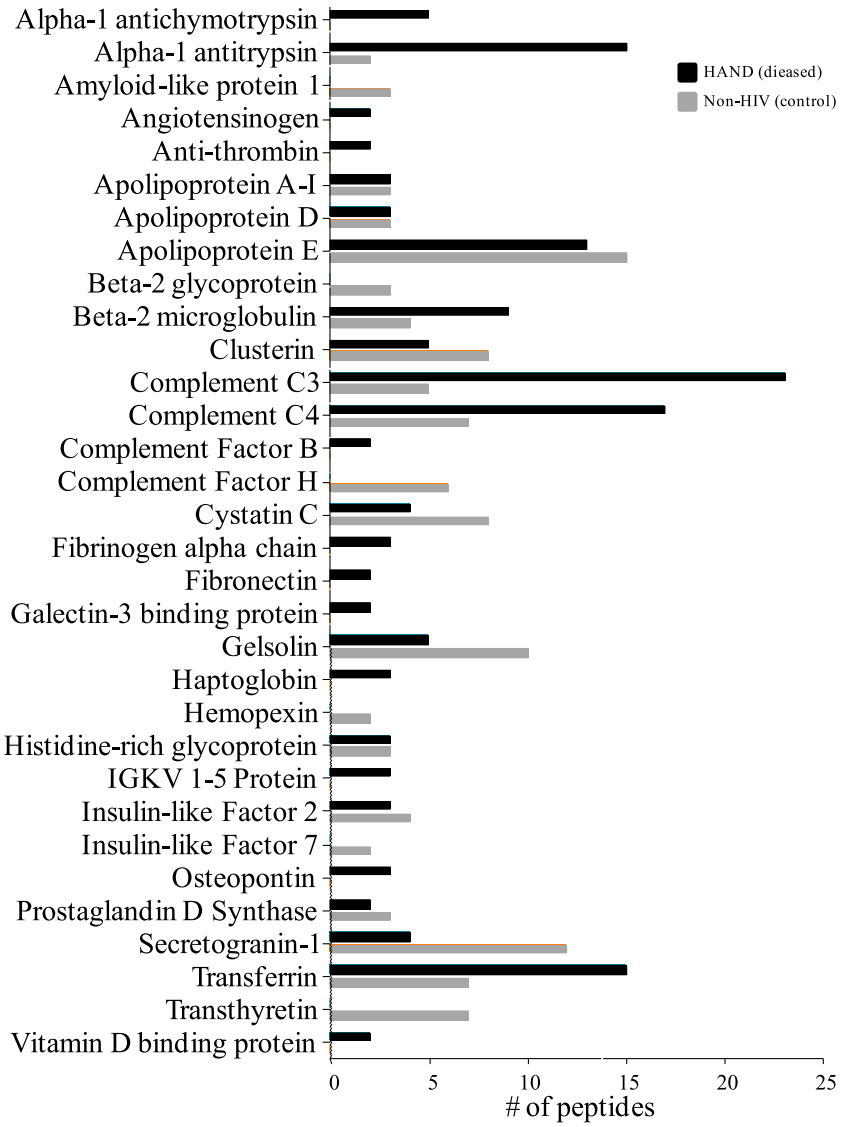

the product ions that were created via CID fragmentation. Two variable modifications were used for both MASCOT and X! Tandem: oxidation of methionine and nitration of tyrosine. The results from MASCOT and X! Tandem were uploaded onto the Scaffold Proteome software (Proteome Software Inc., Portland, OR) to formulate a final protein list. Scaffold Proteome software employs PeptideProphet and ProteinProphet algorithms to generate a bimodal histogram of the correct and incorrect identifications. The algorithms use the histogram to estimate the degree of overlap to determine the probability cutoff for correct peptide identifications. The Scaffold Proteome data sets were annotated and analyzed using ProteinCenter (Proxeon Biosystems, Odense Denmark).

Results

In vitro Nitrotyrosine Results: In vitro n-BSA Model To validate the affinity enrichment of in vitro nitrotyrosine-modified BSA, the antibody-enriched *n*-BSA was analyzed via reversed-phase HPLC (RP-HPLC). The RP-HPLC chromatogram in Fig. 2 displays a peak representative of in vitro *n*-BSA at 214 and 350 nm. Unmodified angiotensin II was added as an internal standard and the angiotensin II peak was present only in the 214 nm chromatogram. The presence of in vitro *n*-BSA at both 214 and 350 nm validates in vitro nitration and affinity enrichment because the peptide bond absorbs at 214 nm and the $–NO_2$ group attached to the tyrosine residue(s) absorbs at 350 nm. The absorbance of unmodified tyrosine is 274 nm; however, the presence of the $–NO_2$ group alters the physical and chemical properties of the tyrosine residue, leading to a shift in UV absorption of tyrosine. Absorption of nitrated tyrosine is pH-dependent, at acidic pH the prominent band of free nitrotyrosine was found to be at 350 nm, which represents the neutral form of nitrotyrosine [10, 11]. However, at basic pH the major band of free nitrotyrosine was found to be at 422 nm, which represents the ionized form of nitrotyrosine (Fig. 2 Inset) [10, 11]. Following RP-HPLC analysis, the co-immunoprecipitation fractions were digested and analyzed by tandem MS via LTQ-Orbitrap. The peptides identified from tryptic digestion of in vitro *n*-BSA are summarized in Table 1, however, few nitrated peptides were observed in the analysis. This may be due to the differential nitration of tyrosine residues on BSA proteins and/or ion suppression during MS/MS analysis. The non-nitrated and nitrated RHPEYAVSVLLR ions were detected in the in vitro *n*-BSA digest (Fig. 3a–c). The detection of both the nitrated and non-nitrated forms of the peptide may stem from the differential nitration of the BSA protein. From the total (normalized) ion chromatogram, the triply charged ion for the non-nitrated (*m/z* 480.61) and nitrated (*m/z* 495.60) form of RHPEYAVSVLLR are present in the selected ion chromatograms (Fig. 3a). Due to the attachment of the $–NO_2$ group on Tyr^{364}, the peptides

Table 3 Identified peptides from tryptic digest of in vivo nitrated L-PGDS from non-HIV (control) and HAND CSF

Peptide sequence	Charge	Mascot Ion Score	Observed m/z	Actual peptide mass (AMU)	Calculated +1H peptide mass (AMU)	Actual minus calculated peptide mass (AMU)
Non-HIV (*n*=3)						
AQGFTEDTIVFLPQTDK	2	54	955.5187	1,909.0228	1,908.9469	0.0759
EKFTAFCKAQGFTEDTIVFLPQTDK	3	35	955.5182	2,863.5328	2,863.4102	0.1225
KNQCETRTM*LLQPAGSLGSYSYR	3	30	873.8182	2,618.4328	2,618.2581	0.1747
SPHWGSTYSVSVVETDYDQYALLYS QGSK	2	41	1,634.174	3,266.3334	3,266.5044	–0.171
SVVAPATDGGLNLTSTFLR	2	132	960.0486	1,918.0826	1,918.016	0.0666
TM*LLQPAGSLGSYSYR	2	68	881.0337	1,760.0528	1,758.8611	1.1918
WFSAGLASNSSWLR	2	20	791.1036	1,580.1926	1,580.7736	–0.5809
HAND (*n*=4)						
AQGFTEDTIVFLPQTDK	2	77	955.4286	1,908.8426	1,908.9469	–0.1043
EKFTAFCKAQGFTEDTIVFLPQTDK	3	42	955.4282	2,863.2628	2,863.4102	–0.1475
KNQCETRTM*LLQPAGSLGSYSYR	3	17	874.1215	2,619.3427	2,618.2581	1.0846
SPHWGSTYSVSVVETDYDQYALLYS QGSK	3	74	1,090.261	3,267.7612	3,266.5044	1.2568
SVVAPATDGGLNLTSTFLR	2	129	959.8787	1,917.7428	1,918.016	–0.2732
TMLLQPAGSLGSYSYR	2	92	872.3737	1,742.7328	1,742.8661	–0.1333
TMLLQPAGSLGSY*SYR	2	50	894.941	1,787.88	1,788.874	–0.994
WFSAGLASNSSWLR	2	20	791.4687	1,580.9228	1,580.7736	0.1493

M*: oxidized methionine; Y*: NO_2-modified tyrosine

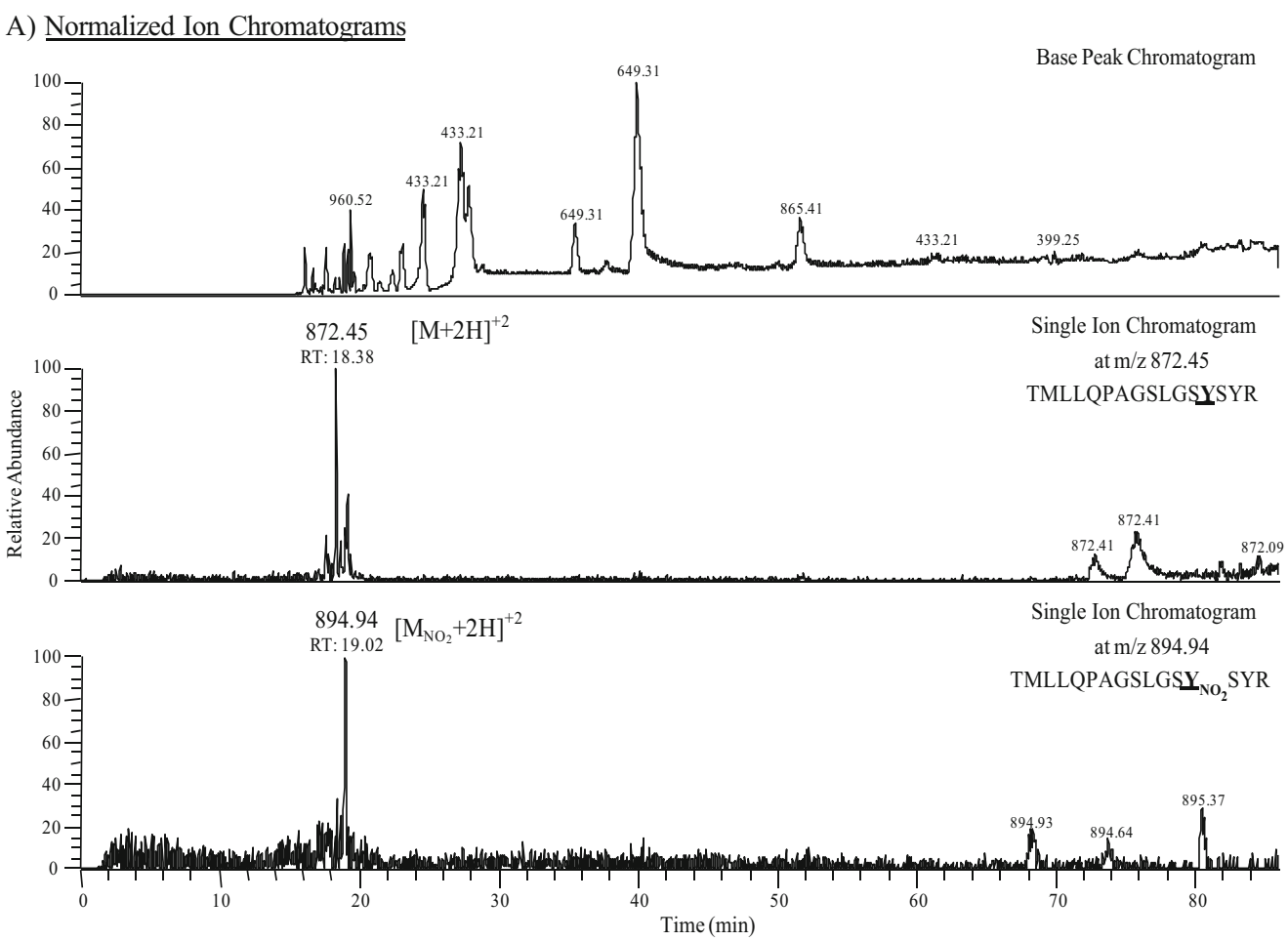

Fig. 5 LTQ-Orbitrap analysis of HAND L-PGDS tryptic peptides: TMLLQPAGSLGS**Y**SYR and TMLLQPAGSLGS**YNO2**SYR. The base peak ion chromatograms of the MS analysis of the tryptic digestion of HAND L-PGDS are presented in Panel A. The single ion chromatograms at *m/z* 872.48 and *m/z* 894.94 represent the detection of the [M+2H]+2 ion of the non-nitrated and nitrated HAND L-PGDS peptide, respectively. The tandem MS spectra of *m/z* 872.48 and *m/z* 894.94 are in Panel B

elute within ~1.0 min of each other. The product ion spectrum for both forms contain relative complete series of b- and y-ions and the difference between b_5/y_8 and $*b_5/*y_8$ fragment ions (asterisks (*) indicate nitrated spectrum) represent the location of the nitrotyrosine modification (Fig. 3c). The nitrotyrosine modification also shifts the immonium ion of tyrosine from *m/z* 136.10 to *m/z* 181.06, as observed in Fig. 3b. The shift in the *m/z* value of the tyrosine immonium ion offers an alternative route to distinguish nitrated peptides from non-nitrated peptides.

In Vivo Nitrotyrosine Results

Nitrotyrosine Sub-proteome of non-HIV and HAND CSF Following albumin/IgG depletion of the pooled CSF samples, slot blot analysis was used to determine the nitrotyrosine content in each sample. We confirmed a higher nitrotyrosine content in the pooled HAND CSF sample compared to the nitrotyrosine present in the non-HIV infected CSF (Fig. 4b). The one-dimensional silver stained images in Fig. 4a represent the fractions from the affinity-based enrichment of both non-HIV and HAND CSF. From tandem MS analysis of the nitrotyrosine-modified tryptic digest products, a total of 32 proteins were identified (Electronic Supplementary Material, Table 1). Of the identified nitrated proteins, nine were unique to non-HIV CSF; eight were unique to HAND CSF; and 15 were observed in both CSF specimens. It is possible that the unique proteins identified in the non-HIV CSF are unique to the underlying disease state of these individuals. Alternatively, since the CSF from HIV-infected individuals were selected for high concentration of nitrated proteins it is possible that these proteins may have masked the other nitrated proteins present in low concentrations. The Scaffold Proteome software was used to evaluate the MS/MS data of the identified proteins from both groups and spectral counting was used as a pseudo-quantification method to determine differential expression of the nitrated proteins. As illustrated in Fig. 4a, there was an increase in the number of

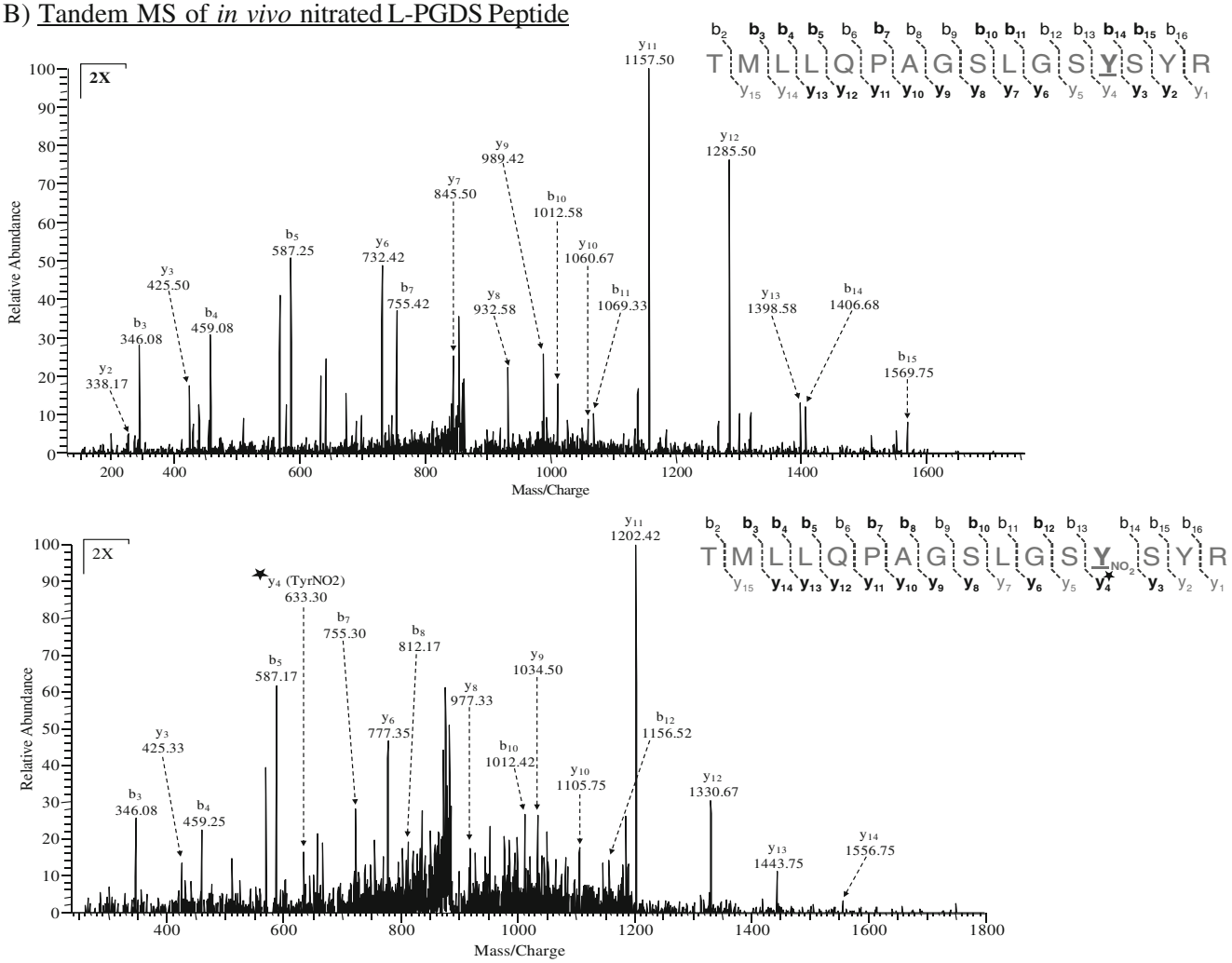

Fig. 5 (continued)

tandem MS spectra observed in the HAND CSF sample when compared to the spectra detected from the non-HIV infected CSF. This suggests that there was a higher concentration of nitrotyrosine-modified proteins in the HAND sample, compared to the non-HIV sample, which is consistent with the slot blot analysis. The bar graph in Table 2 represents the total number of peptides identified per protein in the non-HIV and HAND samples.

In Vivo L-PGDS Analysis from non-HIV and HAND CSF

L-PGDS, also known as β-trace protein, is one of the most abundant brain-derived proteins in human CSF and is primarily expressed in the arachnoid membrane, leptomeninges, and choroid plexus [12]. In addition to expression in the central nervous system, L-PGDS is also expressed in male genital organs, heart, and bodily fluids (plasma, seminal fluid, amniotic fluid, CSF, and urine) [12]. L-PGDS catalyzes the isomerization of prostaglandin-H_2, the precursor to various prostanoids, to prostaglandin-D_2 in the presence of sulfhydryl compounds and also functions as a transporter of small non-substrate lipophilic molecules, including thyroid hormone, retinoic acid, retinaldehyde, bilirubin, and biliverdin [12]. Using the Catch and Release™ system, we were able to isolate nitrotyrosine-modified and unmodified L-PDGS from non-HIV and HAND CSF. The total L-PGDS and nitrotyrosine content from each sample was determined by density analysis of the slot blot images (Fig. 4c). The total L-PGDS content was higher in non-HIV CSF; however the content of in vivo nitrotyrosine-modified L-PGDS was substantially higher in HAND compared to non-HIV. This is possibly due to the increase in nitro-oxidative stress observed in HAND. These findings, however, need to be confirmed in individual samples with larger sample sizes with and without HAND.

In addition to quantitative immunoblot analysis, the enriched L-PGDS was digested with trypsin and analyzed by tandem MS (LTQ-Orbitrap). The peptides identified from each group are presented in Table 3. We did not identify any

nitrated peptides in non-HIV samples; however, the doubly charged non-nitrated (*m/z* 872.44) and nitrated (*m/z* 894.94) TMLLQPAGSLGSYSYR ion was identified in HAND CSF (Fig. 5a). Tandem MS analysis of modified (Fig. 5c) and unmodified (Fig. 5b) TMLLQPAGSLGSY(NO_2)SYR revealed the presence of the $–NO_2$ modification at Tyr^{105} ($*y_4$-ion).

A previous study demonstrated that nitrotyrosine-modified L-PGDS exhibited a loss of enzymatic activity [12]. In this study L-PGDS was in vitro nitrated, which may have lead to extensive nitration of the molecule. However, from our current findings it appears that L-PGDS in CSF of individuals with HAND is nitrated at Tyr^{105}, which is involved in transportation of small lipophilic molecules. Tyr^{105} is a highly conserved residue among members of the lipocalin family and is located in the hydrophobic aromatic cluster of the β-sheet barrel, which is thought to function as the ligand-binding pocket [13]. Structural studies of recombinant mouse L-PGDS reveal that the hydrophobic aromatic cluster plays a major role in the stabilization of retinoic acid [13]. Retinoic acid is an active metabolite of vitamin A and functions as a potent regulator of gene transcription. The stabilization of retinoic acid in the hydrophobic aromatic cluster stems from the relatively strong Van der Waals interactions between the isoprenoid chain and β-ionone ring of retinoic acid and the aromatic ring of Tyr (Tyr^{105} and Tyr^{149}) and Phe (Phe^{34}, Phe^{39}) residues [13]. Nitration of Tyr^{105} alters the physical and chemical characteristics of the residue, including non-covalent and covalent interactions. It has been shown that the addition of the bulky $–NO_2$ group reduces the pKa of the hydroxyl group of Tyr and also introduces steric restrictions to the phenolic ring of Tyr [6].

Therefore, we suggest that nitration of Tyr^{105} disrupts the stabilization of retinoic acid in the hydrophobic binding pocket of L-PGDS. Since L-PGDS is a major component of CSF and highly concentrated in the choroid plexus, which forms the barrier between blood and CSF, it is thought that L-PGDS facilitates the transport of the lipophilic small molecules (e.g., retinoic acid) across the blood/brain barrier [14]. Consequently, interference of the stabilization of retinoic acid as a result of Tyr^{105} nitration in the hydrophobic binding pocket of L-PGDS, could prevent the delivery of retinoic acid to specific target tissues. Previous studies have linked retinoid compounds to the suppression of proinflammatory cytokine and chemokine production during HIV-induced CNS inflammation [15]. Vitamin A deficiency has been associated with enhanced T cell-mediated proinflammatory immune response, which has been shown to contribute to immune-induced tissue damage and also the progression of human disease [15]. It is thought that the HIV infection triggers events that lead to a reduction in plasma levels of vitamin A, which could increase the clinical consequences of HIV infection [15].

Therefore, the inability of nitrotyrosine-modified L-PGDS to transport retinoic acid could potentially lead to the increased progression of the proinflammatory response of HIV-associated neurocognitive dysfunction.

Conclusion

Utilizing immunoaffinity-based enrichment and tandem mass spectrometry we were able to identify and characterize nitrotyrosine-modified proteins from HAND CSF. More specifically, we were able to isolate nitrotyrosine-modified L-PGDS from CSF and characterize the modification site. We conclude from previous structures of mouse L-PGDS, that nitration of Tyr^{105} of L-PGDS can potentially alter its ability to transport retinoic acid, a known regulator of gene expression. A deficiency in vitamin A metabolites has been shown to contribute to the proinflammatory response observed during host invasion (e.g., HIV infection). In addition to its ligand-binding function, L-PGDS also converts prostaglandin-H_2 into prostaglandin-D_2 which is known to play a major role in the inflammatory response, sleep, and also vasodilation. Previous studies have observed elevated levels of prostaglandins in individuals diagnosed with HIV-associated neurocognitive dysfunction [16]. Therefore, further characterization of the influence of nitration on the function of L-PGDS in individuals diagnosed with HAND may lead to the development of potential clinical diagnostics or therapies for HIV-associated neurocognitive dysfunction.

Acknowledgments This work was supported by grants P30 MH075673 (JM) and P20 DA026164 (RJC) from the National Institutes of Health.

References

1. Ghafouri M, Amini S, Khalili K, Sawaya BE. HIV-1 associated dementia: symptoms and causes. Retrovirology. 2006;3:28.
2. Antinori A, Arendt G, Becker JT, Brew BJ, Byrd DA, Cherner M, et al. Updated research nosology for HIV-associated neurocognitive disorders. Neurology. 2007;69(18):1789–99.
3. Ances BM, Ellis RJ. Dementia and neurocognitive disorders due to HIV-1 infection. Semin Neurol. 2007;27(1):86–92.
4. Adamson DC, Wildemann B, Sasaki M, Glass JD, et al. Immunologic NO synthase: elevation in severe AIDS dementia and induction by HIV-1 gp41. Science. 1996;274:1917–20.
5. Ryberg H, Caidahl K. Chromatographic and mass spectrometric methods for quantitative determination of 3-nitrotyrosine in biological samples and their application to human samples. J Chromatogr B Analyt Technol Biomed Life Sci. 2007;851(1–2):160–71.
6. Radi R. Nitric oxide, oxidants, and protein tyrosine nitration. Proc Natl Acad Sci USA. 2004;101:4003–8.
7. Blum H, Beier H, Gross HJ. Improved silver staining of plant proteins. RNA and DNA in polyacrylamide gels. Electrophoresis. 1987;8:93–9.
8. Gharib M, Marcantonio M, Lehmann SG, Courcelles M, et al. Artifactual sulfation of silver-stained proteins: implications for the

assignment of phosphorylation and sulfation sites. Mol Cell Proteomics. 2009;8(3):506–18.
9. Riordan JF, Sokolovsky M, Vallee BL. Environmentally sensitive tyrosyl residues. Nitration with tetranitomethane. Biochemistry. 1967;6:358–61.
10. Dr Filippis V, Frasson R, Fontana A. 3-Nitrotyrosine as a spectroscopic probe for investigating protein-protein interaction. Protein Sci. 2006;15(5):976–86.
11. Lescuyer P, Gandini A, Burkhar PR, Hochstrasser DF, et al. Prostaglandin D2 synthase and its post-translational modifications in neurological disorders. Electrophoresis. 2005;26(23):4563–70.
12. Li W, Malpica-Llanos TM, Gundry R, Cotter RJ, et al. Nitrosative stress with HIV dementia causes decreased L-prostaglandin D synthase activity. Neurology. 2008;70(19 Pt 2):1753–62.
13. Urade Y, Hayaishi O. Biochemical, structural, genetic, physiological, and pathophysiological features of lipocalin-type prostaglandin D synthase. Biochim Biophys Acta. 2000;1482(1–2): 259–71.
14. Flower D. The lipocalin protein family: structure and function. Biochem J. 1996;318:1–14.
15. Royal III W, Vlahov D, Lyles C, Gajewski CD, et al. Retinoids and drugs of abuse: implications for neurological disease risk in human immunodeficiency virus type 1 infection. Clin Infect Dis. 2003;37 Suppl 5:S427–32.
16. Shimamoto S, Yoshida T, Inui T, Gohda K, et al. NMR structure of lipocalin-type prostaglandin D synthase: evidence for partial overlapping of catalytic pocket and retinoic acid-binding pocket within the central cavity. J Biol Chem. 2007;282(43):31373–9.